

# Bulk and shear viscosities of matter created in relativistic heavy-ion collisions

Piotr Bożek<sup>1,2,\*</sup>

<sup>1</sup>*The H. Niewodniczański Institute of Nuclear Physics, PL-31342 Kraków, Poland*

<sup>2</sup>*Institute of Physics, Rzeszów University, PL-35959 Rzeszów, Poland*

(Dated: September 13, 2018)

We study the effects of shear and bulk viscosities in the hadronic phase on the expansion of the fireball and on the particle production in relativistic heavy ion collisions. Comparing simulation with or without viscosity in the hadronic matter we find that elliptic flow observables strongly dependent on dissipative effects in the late stage. On the other hand, interferometry radii are sensitive, through the early transverse flow, on the value of the viscosity at high temperatures. We present first calculations including the effects of bulk viscosity in the hadronic phase and in the hadron emission. We find them important in obtaining a small freeze-out temperature consistent with the measured transverse momentum spectra and elliptic flow of identified particles.

PACS numbers: 25.75.-q, 25.75.Dw, 25.75.Ld

Keywords: relativistic heavy-ion collisions, viscous hydrodynamic model, collective flow

## I. INTRODUCTION

The matter created in relativistic heavy-ion collisions at the BNL Relativistic Heavy Ion Collider (RHIC) is a dense strongly interacting fluid [1–4]. The observation of strong collective transverse and elliptic flows is an indication that the system behaves as a fluid. To model the dynamics of such a system relativistic hydrodynamics of a perfect fluid has been successfully applied [5–11]. The fireball expands and cools down, until some freeze-out temperature is reached, after which particles are emitted from a freeze-out hypersurface. Final particle spectra, to be compared with experimental data, are obtained after resonance decays. Transverse momentum spectra in the azimuthal angle at central rapidity are written as an expansion in Fourier coefficients

$$\frac{dN}{d^2p_{\perp}dy} = \frac{dN}{2\pi p_{\perp}dp_{\perp}dy} (1 + v_2 \cos(2\phi) + \dots) . \quad (1.1)$$

The form of the observed transverse momentum spectra  $\frac{dN}{2\pi p_{\perp}dp_{\perp}dy}$  and the elliptic flow coefficient  $v_2$  can be described using a convolution of the thermal emission of particles with the collective velocity of the fluid itself [12, 13].

Due to the rapid expansion of the dense system created in relativistic heavy-ion collisions deviations from local equilibrium can be important. For the modeling of the expansion of the fireball it means that viscous relativistic hydrodynamics should be used [14–19]. A consistent causal scheme requires the use of second order viscous equations [20]. Most of the existing applications of viscous hydrodynamics in heavy-ion collisions consider shear viscosity only. The value of the ratio  $\eta/s$  of the shear viscosity coefficient to the entropy density is an important characteristic of the strongly interacting medium

created in the course of the collision [21, 22]. The extraction of the shear viscosity coefficient from the measured elliptic flow could give valuable information [17, 23]. The main source of uncertainty in the analysis lies in the assumption of the initial eccentricity of the source at a given impact parameter [23]. The causes influencing the initial shape of the source include : different underlying models of the initial density, Color Glass Condensate or Glauber Model [24], the inclusion of binary collision contributions [25], possible initial fluctuations of the shape (standard versus participant eccentricity) [26, 27] or a core-corona effect, where only the dense part of the source evolves collectively [28]. The elliptic flow of the bulk of the matter is generated in the early stages of the collision. However, the final elliptic flow of observed hadrons is modified in the hadron gas phase of the expansion, due to rescattering and resonance decays [10, 29–31]. This is true both for the elliptic flow of charged particles as well as of identified particles [10, 32]. In particular, to reproduce the observed splitting between pions and protons in the transverse momentum dependence of  $v_2$  a late freeze-out or a hadronic cascade stage are required in the evolution.

The role of dissipation in the hadronic phase must be assessed before a reliable estimate of viscosity in the (quark-gluon plasma) QGP phase can be made. Although the importance of the difference of the viscosity coefficients in the hadronic and plasma phases has been discussed [29], most of the existing hydrodynamic simulations applied to heavy ion collisions use a constant  $\eta/s$  ratio through the evolution. In this paper we study the effect of viscosity in the hydrodynamic evolution below the transition temperature on the final elliptic flow, spectra and Hanbury Brown-Twiss (HBT) correlation radii. In particular we analyze the observable differences in soft momenta observables between two extreme assumptions on the shear viscosity in the plasma phase ( $\eta/s = 0$  or 0.16), after hadronic dissipation is taken into account. We show that the effect of dissipation in the hadronic phase strongly reduces the sensitivity of the elliptic flow

\*Electronic address: [Piotr.Bozek@ifj.edu.pl](mailto:Piotr.Bozek@ifj.edu.pl)

measure on the value of the viscosity in the early QGP phase of the expansion. If the hadronic phase in the expansion is dilute enough, a cascade after burner can be used after an early freeze-out of the fluid [31, 33–35]. Alternatively a longer hydrodynamic evolution can be used with a hadronic equation of state below the transition temperature. This paper studies the effect of such a longer hydrodynamic evolution in the hadronic phase using viscous hydrodynamics. We use a moderate value of  $\eta/s = 0.1$  in the hadronic phase and a bulk viscosity  $\zeta/s = 0.03-0.04$ . We show that even such small values of viscosities in the hydrodynamic evolution in the late phase of the collision are important for the final elliptic flow, and that with such assumptions we can reproduce many experimental observations. We calculate also the HBT radii after a hydrodynamic evolution with different viscosities in the QGP and hadron gas phases.

## II. SHEAR AND BULK VISCOSITIES

Besides the ideal fluid expansion we consider three other scenarios for the shear and bulk viscosities in the hot matter. The general idea is that the shear viscosity in the hadronic and QGP phases could be very different. Moreover if the shear viscosity in the hadronic phase is non-zero, it could be accompanied by non-negligible bulk viscosity. The formula for the temperature dependence of the ratio of the shear viscosity to the entropy is taken in the form

$$\frac{\eta}{s}(T) = f_{low}(T) \frac{\eta_{HG}}{s} f_{HG}(T) + (1 - f_{HG}(T)) \frac{\eta_{QGP}}{s} \quad (2.1)$$

where the function  $f_{HG}(T) = 1/(\exp((T - T_c)/\Delta T) + 1)$  cuts-off the hadron gas viscosity above  $T_c = 170\text{MeV}$  ( $\Delta T = 8\text{MeV}$ ).  $f_{low}(T) = 1/(\exp((T_{low} - T)/\Delta T) + 1)$  is introduced to cut-off viscosity effects below  $T_{low} = 80\text{MeV}$  to improve numerical stability. Depending on the chosen values of the viscosities in the hadronic matter and in QGP we consider four different scenarios (Table I). The temperature dependence of the viscosities corresponding to viscous scenarios in the Table are shown in Fig. 1. The scenario denoted as vHG assumes that only viscosity in the hadronic phase is non-zero. vQGP is taken for illustration to show how the dissipative phenomena in the plasma alone could influence the final observables. The scenario vQGP+vHG is the most general (with a suitable choice of  $\eta_{HG}$  and  $\eta_{QGP}$ ). The two scenarios vHG and vQGP+vHG differ by the choice of the shear viscosity coefficient in the plasma. The comparison of these two different scenarios is one of the motivations of this investigation, namely to test how sensitive the final observables are to the assumed viscosity in the plasma phase (from  $\eta/s = 0$  to  $\eta/s = 0.16$ ), when dissipation in the hadronic phase occurs afterwards. These two scenarios represent two extreme assumptions on the temperature dependence of the ratio  $\eta/s$ , i.e.

acronym	$\frac{\eta_{HG}}{s}$	$\frac{\eta_{QGP}}{s}$	$T_F$ (MeV)
id. fl.	0	0	140
vHG	0.1	0	150
vQGP	0	0.16	130
vHG+vQGP	0.1	0.16	135

TABLE I: Viscosity parameters used in the four calculations presented in the paper. The last column contains the freeze-out temperature that reproduces best pion spectra in each case.

increasing or decreasing when switching from the QGP to hadronic matter. Existing viscous hydrodynamic simulations assume a constant  $\eta/s$  as function of temperature, microscopic estimates suggest a (strong) increase of  $\eta/s$  when decreasing the temperature. We test a scenario with a moderate increase of  $\eta/s$  at  $T_c$  and also another extreme scenario where the reverse happens and show that the results are in fact very similar and that reproducing experimental data requires a small value of  $\eta_{HG}$  for any QGP viscosity.

The near equilibrium regime in a dilute gas of interacting hadrons can be described using the Boltzmann equation. Estimates of shear viscosity with hadronic cross sections or chiral models lead to a large value  $\eta/s \simeq 1$  for temperatures  $T \simeq 150\text{MeV}$  [36–40]. The large value  $\eta/s \simeq 1$  in the hadronic phase seems to contradict existing fits of the data using viscous hydrodynamics, where  $\eta/s = 0.08-0.16$  depending on the initial eccentricity [17]. Also such a large value of the viscosity coefficient would simply mean that the viscous hydrodynamics cannot be applied. Shear viscosity could be significantly reduced if the number of hadronic states increases near  $T_c$  [41]. At temperatures close to the transition temperature the description of the dense medium using a transport equation approach involving hadrons with vacuum properties could break down. On the other hand, in microscopic models the bulk viscosity is estimated to be much smaller  $\zeta/s \simeq 0.03-0.05$  [41, 42].

In this paper, we use relativistic viscous hydrodynamics to model the dense hot medium on the low temperature side of the transition temperature. The equation of state of matter for  $T < T_c$  is approximated as the hadron gas equation of state involving 371 known hadrons and resonances [43]. This equation of state can be smoothly connected to the equation of state calculated in lattice QCD at higher temperatures. The final equation of state leads to a correct description of spectra and HBT radii in ideal fluid hydrodynamics [11, 44]. Shear viscosity in the hadronic phase is treated as a free parameter in our calculation. A simple estimate of the viscosities can be obtained in the relaxation time approximation [45–47]. Starting from the Boltzmann equation for the phase space distribution  $f_n$  of particle species  $n$

$$p^\mu \partial_\mu f_n = -\frac{p^\mu u_\mu(x) \delta f_n}{\tau_{HG}} \quad (2.2)$$

where  $\delta f_n = f_n - f_n^0$  is the deviation from the equilibrium (Bose-Einstein or Fermi-Dirac) distribution  $f_n^0 = \frac{1}{\exp(p^\mu u_\mu(x)/T) \pm 1}$ ,  $u_\mu(x)$  is the local fluid four-velocity, and  $\tau_{HG}$  is the relaxation time (the same for all particle species). In the local rest frame we have

$$\delta f_n = \frac{\tau_{HG}}{TE} f_n^0 (1 \pm f_n^0) (p^i p^j \partial_i v^j - c_s^2 E^2 \partial_i v^j) . \quad (2.3)$$

Calculating the stress corrections to the energy momentum tensor

$$\delta T^{\mu\nu} = \pi^{\mu\nu} + \Pi \Delta^{\mu\nu} = \sum_n \int \frac{d^3 p}{(2\pi)^3 E} p^\mu p^\nu \delta f_n , \quad (2.4)$$

where  $\Delta^{\mu\nu} = g^{\mu\nu} - u^\mu u^\nu$ , we get for the stress tensor in the local rest frame

$$\pi^{ij} = \frac{\tau_{HG}}{T} \sum_n \int \frac{d^3 p}{(2\pi)^3} \frac{p^i p^j p^k p^l}{E^2} f_n^0 (1 \pm f_n^0) \sigma^{kl} \quad (2.5)$$

and

$$\Pi = \frac{\tau_{HG}}{T} \sum_n \int \frac{d^3 p}{(2\pi)^3} \frac{m^3}{3E^2} f_n^0 (1 \pm f_n^0) \left( \frac{p^2}{3E} - c_s^2 E \right) \nabla \mathbf{u} \quad (2.6)$$

with

$$\sigma_{\alpha\beta} = \frac{1}{2} \left( \nabla_\alpha u_\beta + \nabla_\beta u_\alpha - \frac{2}{3} \Delta_{\alpha\beta} \partial_\mu u^\mu \right) . \quad (2.7)$$

Comparing with the first order expressions for the stress tensor  $\pi_{\mu\nu} = 2\eta\sigma_{\mu\nu}$ ,  $\Pi = -\zeta\partial_\mu u^\mu$  we have

$$\eta = \frac{1}{15T} \sum_n \int \frac{d^3 p}{(2\pi)^3} \frac{p^4}{E^2} f_n^0 (1 \pm f_n^0) \quad (2.8)$$

and

$$\zeta = \frac{\tau_{HG}}{3T} \sum_n \int \frac{d^3 p}{(2\pi)^3} \frac{m^2}{E} f_n^0 (1 \pm f_n^0) \left( c_s^2 E - \frac{p^2}{3E} \right) . \quad (2.9)$$

In the modelling of heavy ion collisions we are interested in the properties of the hadronic matter in a temperature range from the freeze-out temperature  $T_F > 130\text{MeV}$  to the transition temperature  $T_c = 170\text{MeV}$ . Performing the sums over the resonances used in the calculation of the hadronic matter equation of state, i.e. the resonances listed in the SHARE program [48], we can relate the viscosity coefficient to the relaxation time. Assuming a constant shear viscosity to entropy ratio  $\eta/s = 0.1$  between 80 and 170MeV, the relaxation time  $\tau_{HG}$  changes weakly in the range 0.8-1.2fm/c. We could assume instead a different dependence of  $\eta/s$  or of  $\tau_{HG}$  on the temperature, but these details do not matter much. It turns out that it is the value at freeze-out that is the most important. Our choice corresponds to  $\tau_{HG} \simeq 1\text{fm}/c$  at  $T = 150\text{MeV}$ , but other values of the parameters could be tested in more extensive sets of model

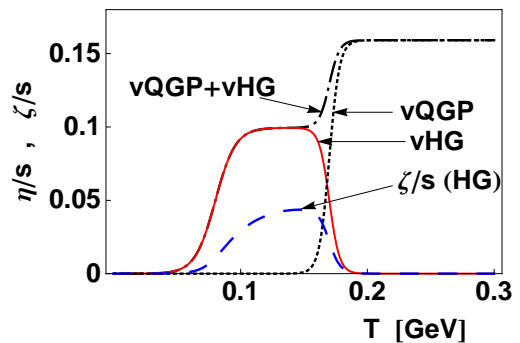


FIG. 1: (Color online) Temperature dependence of the ratio of shear and bulk viscosities to the entropy. The solid, dotted and dash-dotted lines represent the shear viscosity for the vHG, vQGP and vQGP+vHG scenarios. The dashed line represent the bulk viscosity, effective only in the vHG and vQGP+vHG scenarios.

calculations. The assumed small hadronic shear viscosity is not motivated by microscopic model estimates, that would suggest a larger value. It is rather motivated by existing viscous hydrodynamic calculations [17, 23], indicating that the average viscosity in the hadronic and QGP phases is small.

The bulk viscosity of the hadronic matter at high density is another not very well controlled parameter. It is expected that in the deconfined phase the bulk viscosity coefficient is negligible. On the other hand, a sharp rise of the bulk viscosity has been predicted [49] around  $T_c$ . If the effect of the bulk viscosity at  $T_c$  is large the flow could be modified [50, 51] or could even become unstable leading to the fragmentation of the fireball [52]. On the other hand, the rise of the bulk viscosity near  $T_c$  could be accompanied by critical slowing down, which leads to an increase of the dynamical bulk viscosity relaxation time  $\tau_\Pi$ , delaying the onset and effectively diminishing bulk viscosity effects. 2 + 1D hydrodynamic simulations indicate that by the time the expanding system reaches  $T_c$  substantial amount of transverse flow has already set in [50] and the effects of the rising bulk viscosity at the critical temperature is reduced and the agreement of the calculation with the data is not spoiled. In this paper we do not take into account bulk viscosity near the phase transition.

In the hadron gas phase the bulk viscosity could be quite substantial, as particle masses get comparable to the temperature. Bulk viscosity can be estimated in the relaxation time approximation from Eq. (2.9). The resulting  $\zeta/s$  corresponding to  $\eta_{HG}/s = 0.1$  is shown in Fig. 1. Since the relaxation time formulas use physical hadrons, we restrict the temperature range for the calculation in Eqs. 2.8 and 2.9 to the hadronic phase, taking  $\frac{\eta}{s}(T) = f_{low}(T) \frac{\eta_{HG}}{s} f_{HG}(T)$ . The shear viscosity at larger temperatures  $(1 - f_{HG}(T)) \frac{\eta_{QGP}}{s}$  is not generated through hadronic processes. In this paper we are interested in the effects of bulk viscosity in the late stages, and therefore we do not take into account possible bulk

viscosity of non-hadronic origin. At temperatures around 150MeV we have  $\zeta/s \simeq 0.035$ . For our estimate of viscosities using a relaxation time formula with  $\tau_{HG}$  of the order of 1fm/c we obtain the bulk viscosity similar as in microscopic models [42] but the shear viscosity is significantly smaller than in most estimates [36–40]. To check this assumption we performed also a calculation with the same bulk viscosity but increasing  $\eta_{HG}/s$  to 0.24. This would mean that relaxation time formulas do not apply. We find that the assumed value of the shear viscosity  $\eta_{HG}/s = 0.24$ , which is still smaller than microscopic estimates, gives already a too strong suppression of the elliptic flow.

Eq. (2.2) defines nonequilibrium corrections to the distribution function. The corrections from bulk viscosity cannot be taken in the form of the Grad's expansion [53]. From Eq. (2.2) we get for the corrections from bulk viscosity  $\Pi$  [47]

$$\delta f_n^{bulk} = C_{bulk} f_n^0 (1 \pm f_n^0) \left( c_s^2 E - \frac{p^2}{3E} \right) \Pi \quad (2.10)$$

in the local rest frame, with

$$\frac{1}{C_{bulk}} = \frac{1}{3T} \sum_n \int \frac{d^3p}{(2\pi)^3} \frac{m^2}{E} f_n^0 (1 \pm f_n^0) \left( c_s^2 E - \frac{p^2}{3E} \right). \quad (2.11)$$

The deviation from equilibrium due to the stress corrections from shear viscosity are taken in the form [15, 54]

$$\delta f_{shear} = f_n^0 (1 \pm f_n^0) \frac{1}{2T^2(\epsilon + p)} p^\mu p^\nu \pi_{\mu\nu} \quad (2.12)$$

with  $\epsilon$  the local energy density and  $p$  the pressure. It must be noted that more general forms of the nonequilibrium corrections are possible for multicomponent systems or for species dependent relaxation times [55].

### III. VISCOUS HYDRODYNAMIC EVOLUTION

The hydrodynamic equations

$$\partial_\mu T^{\mu\nu} = 0 \quad (3.1)$$

are solved in 2 + 1 dimensions, assuming boost invariance in the longitudinal direction. The energy momentum tensor

$$T^{\mu\nu} = (\epsilon + p)u^\mu u^\nu - pg^{\mu\nu} + \pi^{\mu\nu} + \Pi\Delta^{\mu\nu} \quad (3.2)$$

is composed of the ideal fluid part and stress shear and bulk viscosity corrections  $\pi$  and  $\Pi$ . The viscous corrections in the second order Israel-Steward viscous hydrodynamics are solutions of the dynamical equations [20]

$$\Delta^{\mu\alpha} \Delta^{\nu\beta} u^\gamma \partial_\gamma \pi_{\alpha\beta} = \frac{2\eta\sigma^{\mu\nu} - \pi^{\mu\nu}}{\tau_\pi} - \frac{1}{2}\pi^{\mu\nu} \frac{\eta T}{\tau_\pi} \partial_\alpha \left( \frac{\tau_\pi u^\alpha}{\eta T} \right) \quad (3.3)$$

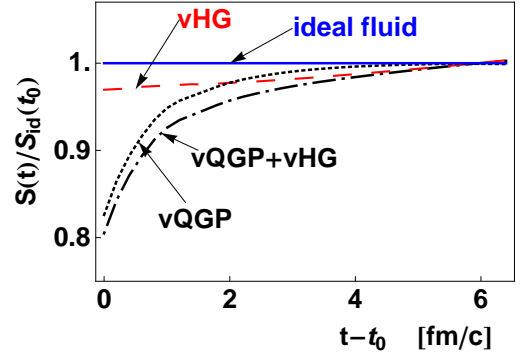


FIG. 2: (Color online) Time dependence of the entropy scaled by the initial entropy in the ideal fluid calculation. The solid, dashed, dash-dotted and dashed lines represent results from the ideal fluid, vQGP, vQGP+vHG and vHG calculations respectively.

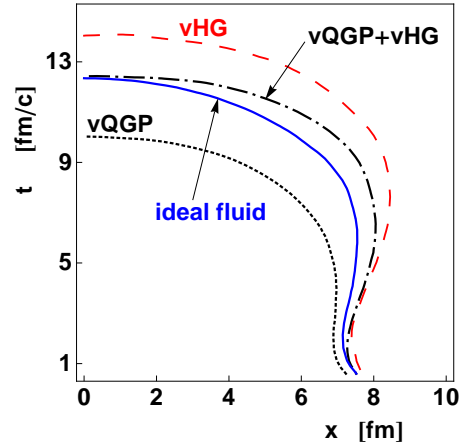


FIG. 3: (Color online) Freeze-out hypersurfaces  $T(t, x, y = 0) = T_F$  at impact parameter  $b = 2.2\text{fm}$ . The solid, dashed, dash-dotted and dashed lines represent hypersurfaces in the ideal fluid, vQGP, vQGP+vHG and vHG calculations respectively.

and

$$u^\gamma \partial_\gamma \Pi = \frac{-\zeta \partial_\gamma u^\gamma - \Pi}{\tau_\Pi} - \frac{1}{2} \Pi \frac{\zeta T}{\tau_\Pi} \partial_\alpha \left( \frac{\tau_\Pi u^\alpha}{\zeta T} \right). \quad (3.4)$$

We take for the relaxation time  $\tau_\pi = \frac{3\eta}{T_s}$ , and assume  $\tau_\Pi = \tau_\pi$ . The initial conditions are  $\pi^{xx}(\tau_0) = \pi^{yy}(\tau_0) = \frac{2\eta}{3\tau_0}$ ,  $\pi^{xy}(\tau_0) = 0$  and  $\Pi(\tau_0) = 0$ . The details of the choice of initial conditions and  $\tau_\Pi$  are not crucial, as the bulk viscosity correction gets rapidly close to the Navier-Stokes value, and anyway its influence on the dynamics itself is small.

For the energy density profile in the transverse ( $x$ - $y$ ) plane at impact parameter  $b$  we use the Glauber Model density

$$\epsilon(x, y, b) = \epsilon_0 \frac{(1 - \alpha)\rho_{WN}(x, y, b) + 2\alpha\rho_B(x, y, b)}{(1 - \alpha)\rho_{WN}(0, 0, 0) + 2\alpha\rho_B(0, 0, 0)} \quad (3.5)$$

where  $\rho_{WN}$  and  $\rho_B$  are the densities of wounded nucleon and binary collisions respectively,  $\alpha = 0.145$ . The optical Glauber Model densities are obtained with Wood-Saxon densities for the Au nuclei  $\rho_{WS}(r) = \rho_0 / (\exp((r - R_a)/a) + 1)$  ( $\rho_0 = 0.169\text{fm}^{-3}$ ,  $R_a = 6.38\text{fm}$ ,  $a = 0.535\text{fm}$ ) and the inelastic cross section is  $42\text{mb}$ . The energy density at the center of the fireball  $\epsilon_0$  for  $b = 0$  is adjusted to reproduce the particle multiplicity in the most central (0-5%) collisions in ideal hydrodynamic simulations. The initial density for other centralities is taken from the formula (3.5) without changing any parameters. In viscous hydrodynamic calculations the initial density is rescaled to take into account the additional entropy produced. In Fig. 2 is shown the entropy production in the different hydrodynamic evolutions. The entropy is normalized to the entropy in the ideal fluid simulation. In viscous hydrodynamics the entropy increases with time, we chose to normalize the entropy in all the calculations to the same value at  $\tau - \tau_0 = 6\text{fm}/c$ . This procedure yields, after hadronization, similar particle multiplicities in all the calculations. Entropy is produced mainly in the QGP phase  $\Delta S/S \simeq 20\%$ , whereas in the hadronic matter its relative increase is only 2-3%.

The freeze-out temperature is fixed to reproduce the transverse momentum spectra of pions in central collisions. The lifetime of the fireball is determined by the initial temperature, the expansion rate and the freeze-out temperature. The interplay of those effects makes the lifetime in the ideal fluid and vQGP+vHG scenarios very similar. The detailed shape of the freeze-out hypersurface depends however on the amount of the accumulated transverse flow (Fig. 3). This has consequences on the resulting HBT radii and in particular on the ratio  $R_{out}/R_{side}$ .

#### IV. RESULTS

Transverse momentum spectra of pions are shown in Fig. 4. The freeze-out temperature is adjusted for each of the considered scenarios to reproduce pion spectra in the most central collisions for  $p_{\perp} < 1.2\text{GeV}/c$ . In the ideal fluid expansion, reducing the freeze-out temperature means that the fluid expands longer and more transverse flow builds up. This effect dominates over the reduction of the final temperature and the spectra become harder. For the chosen initial conditions,  $T_F = 140\text{MeV}$  is optimal for the ideal fluid expanding from  $\tau_0 = 0.6\text{fm}/c$ . Shear viscosity corrections in the plasma phase (scenario vQGP) result in additional transverse pressure in the early stage of the expansion. To reproduce the observed pion spectra the evolution must be shortened giving  $T_F = 150\text{MeV}$ . The situation is very different if dissipative corrections in the hadronic phase are allowed for (scenarios vHG or vQGP+vHG). Bulk viscosity leads to a substantial softening of light particle spectra, hydrodynamic evolution must be effective for a

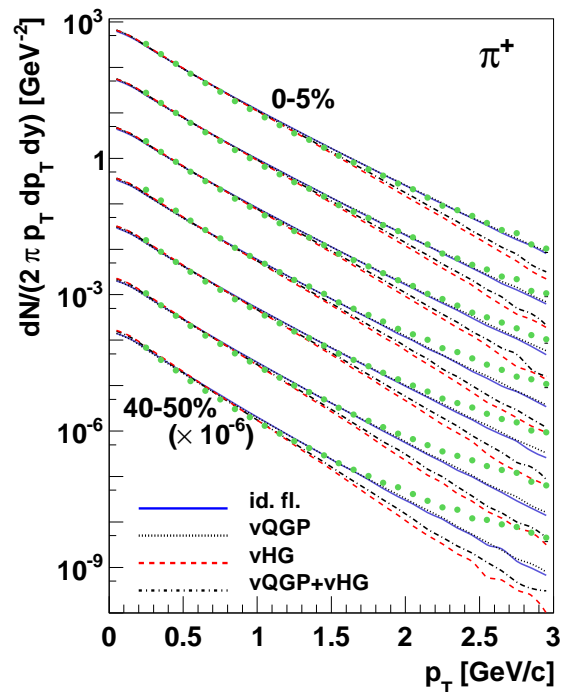


FIG. 4: (Color online)  $\pi^+$  transverse momentum spectra spectra for Au-Au collisions at  $\sqrt{s} = 200\text{GeV}$  and centralities 0-5%, 5-10%, 10-15%, 15-20%, 20-30%, 30-40% and 40-50% (successively scaled down by powers of 0.1). The solid, dotted, dashed and dash-dotted lines represent the results of ideal hydrodynamic, vQGP, vHG and vQGP+vHG calculations respectively. Data are from PHENIX Collaboration [56].

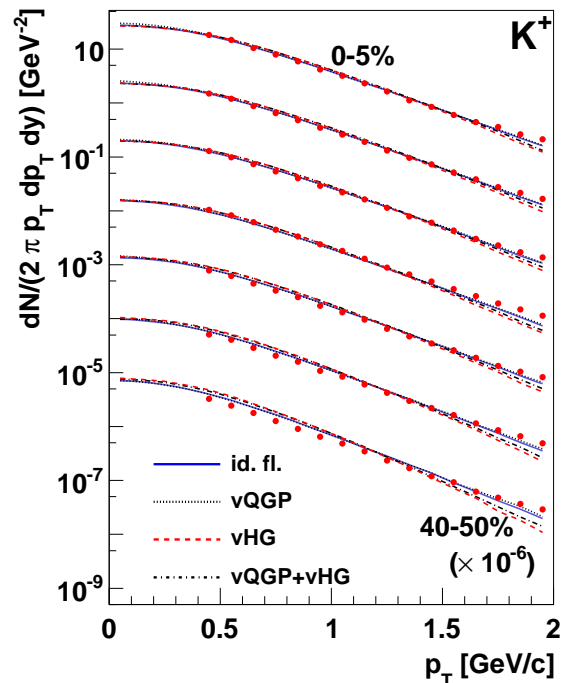


FIG. 5: (Color online) Same as Fig 4 but for  $K^+$ .

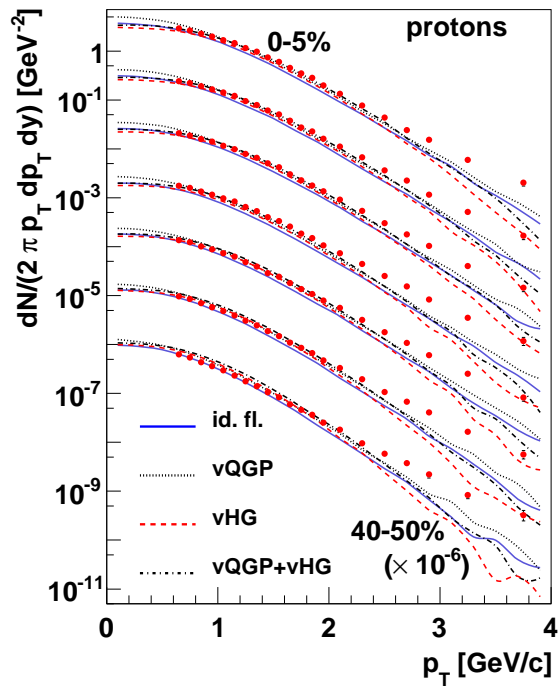


FIG. 6: (Color online) Same as Fig 4 but for protons.

longer time in order to reproduce the  $p_{\perp}$  spectra of pions. Depending on the amount of collective transverse flow accumulated in the early phase of the dynamics it results in freeze-out temperatures 130-135MeV. Bulk viscosity corrections (Eq. 2.11) grow with the momentum of the particle and eventually become as large as the equilibrium distribution  $f^0$ , it means that the formalism breaks down. Using the average bulk viscosity corrections at the freeze-out hypersurface we estimate that viscous hydrodynamics with statistical emission of particles breaks down for pion momenta of 1.5GeV/c in the fluid rest frame. Pion spectra at large transverse momenta cannot be reliably described in the formalism used in this work. After adjusting the freeze-out conditions to reproduce pion spectra at soft momenta in central collisions, all observables at different centralities are calculated without modifying the parameters of the model. We observe that pion spectra at different centralities are well described for  $p_{\perp} < 1.2\text{GeV}/c$ .

In Figs. 5 and 6 we show the spectra of  $K^+$  and protons at different centralities. A first observation is that the slopes of the spectra for heavier particles obtained in scenarios with or without bulk viscosity do not differ as much as for pions. It is a consequence of the mass dependence of the bulk viscosity corrections in Eq. (2.11). Kaon production is overpredicted by hydrodynamic calculations in peripheral collisions which may be a manifestation of partial equilibration of strangeness [58] or of a nontrivial dependence of the thermal source size on centrality [59, 60]. The effective slopes of proton spectra for  $p_{\perp} < 2\text{GeV}/c$  are well reproduced by all the calculations. The multiplicity of protons, reflected in the normaliza-

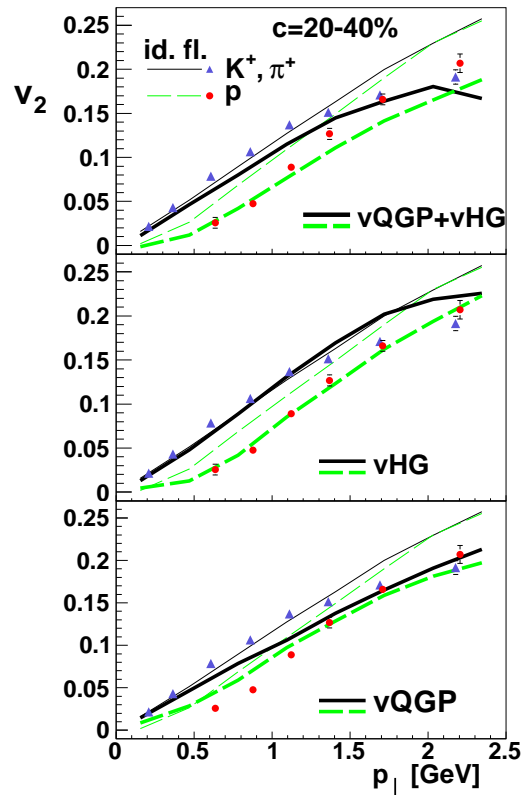


FIG. 7: (Color online) Elliptic flow coefficient for  $\pi^+$  and  $K^+$  (triangles and solid lines) and for protons (circles and dashed lines). Thin lines are for the ideal fluid model (all panels) and the thick lines for the various viscous hydrodynamic calculations, data are from the PHENIX Collab. [57]. In the upper, middle and lower panel are shown results obtained from vQGP+vHG, vHG and vQGP scenarios respectively.

tion of the spectra in Fig. 6, is better described if bulk viscosity is present. The chemical freeze-out temperature fitted from the particle number ratios is 165MeV [61, 62], significantly larger than the freeze-out temperatures we use. Simulations where particles are emitted without bulk viscosity corrections (id. fl. or vQGP) underpredict the number of heavier particles. Bulk viscosity corrections reduce the number of light particles and lead to an increase in heavy particle production, resulting in an effective chemical non-equilibrium at freeze-out. Consequently, simulations including moderate bulk viscosity in the hadronic stage reproduce the proton number in spite of lower freeze-out temperatures.

An important characteristic of the dynamics and of the equation of state of the fireball is the elliptic flow coefficient [6]. Most of the elliptic flow is created in the early phase of the expansion, and so the flow probes pressure gradients at that time. However at densities where freeze-out occurs the elliptic flow is still increasing during the hydrodynamic evolution. Extracting the shear

viscosity from the comparison of model calculations to the data requires a very precise, independent determination of the freeze-out time. A strong constraint on the final density at freeze-out is given by the transverse momentum dependence of  $v_2$  for different species [32] and in particular the difference in the flow of pions and protons. This picture is more complicated if viscosity corrections at freeze-out are important. First, non-equilibrium corrections from shear viscosity could in principle be very different for different particles [55] and second, bulk viscosity corrections (Eq. 2.11) depend on the particle mass.

In Fig. 7 we show the momentum dependent elliptic flow coefficient for light mesons and protons. The ideal fluid simulation (thin lines in all the panels) does not reproduce the meson-proton splitting present in the data. The elliptic flow of protons is too large. The same is true for the scenario where the viscosity is negligible in the hadronic phase (lower panel). Nonequilibrium corrections at freeze-out (both from shear and bulk viscosities) are essentially zero in that case. Shear viscosity in the plasma phase changes the flow pattern reducing velocity gradients and leading to a decrease of the final elliptic flow. Meson and proton elliptic flow gets reduced in a similar way by the shear viscosity, and we cannot get enough meson-proton splitting. The situation is very different if we allow for viscosity corrections in the final stage of the expansion. The most important difference comes from corrections to the distribution functions at freeze-out. Shear viscosity corrections lead to an additional reduction of the elliptic flow. However, bulk viscosity corrections reduce the transverse momenta of light mesons and the differential elliptic flow in  $p_\perp$  is increased (two upper panels in Fig. 7). The same effect has been noticed in the estimates of bulk viscosity corrections at freeze-out in Ref. [53]. Bulk viscosity corrections are much smaller for heavy particles and are not sufficient to increase the value of the elliptic flow for protons. This and the lower freeze-out temperatures in the scenarios with hadronic bulk viscosity bring the species dependent elliptic flow to an agreement with the data.

An interesting experimental observation is the mass scaling of identified particle elliptic flow in transverse mass [63] at small momenta. The mass ordering of the elliptic flow indicates a hydrodynamic origin of the observed flow. In Fig. 8 we present the elliptic flow as function of transverse mass for several identified hadrons. The results for different centralities are scaled by the initial eccentricity of the fireball. The results in different panels correspond to different scenarios for the viscosities. The best agreement with the transverse mass scaling is seen in the calculations with small freeze-out temperatures, vHG or vQGP+vHG. Our calculations in the ideal fluid or vQGP scenarios cannot reproduce the observed mass ordering. It must be noted that ideal fluid simulations with low freeze-out temperatures capture correctly the hydrodynamic origin of the mass ordering of the flow [65]. Similar results are obtained in hydrodynamics with shear viscosity for one value of  $\eta/s$  [66].

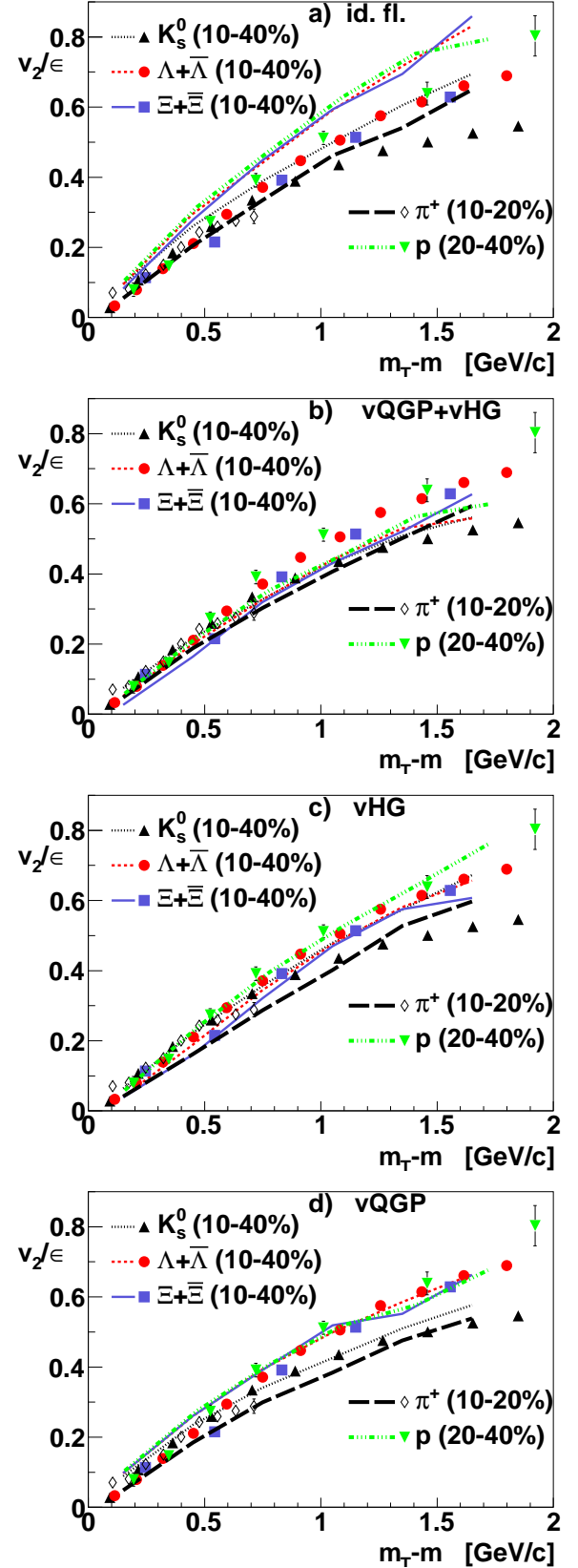


FIG. 8: (Color online) Elliptic flow as function of transverse mass from hydrodynamic calculation (scaled by the initial eccentricity in the calculation, lines) and observed experimentally (scaled by the participant eccentricity, symbols) for  $K_s^0$  (triangles and dotted line),  $\Lambda+\bar{\Lambda}$  (circles and short dashed line),  $\Xi+\bar{\Xi}$  (squares and solid line), all at centralities 10–40%, STAR Collab. data [63], for  $\pi^+$  at centralities 10–20% (diamonds and long dashed line), PHENIX Collab. data [57], and for protons at centralities 20–40% (reversed triangles and dash-dotted line), STAR Collab. data [64].

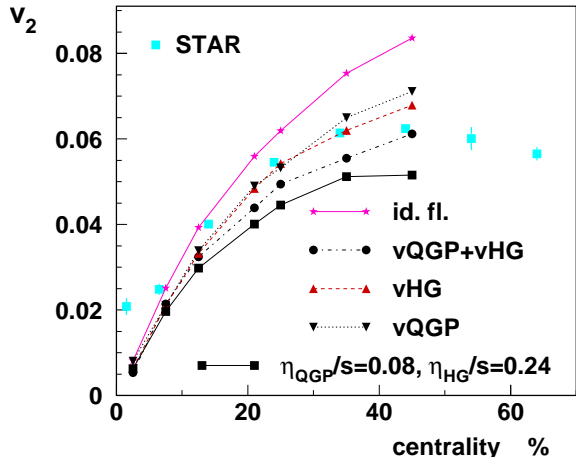


FIG. 9: (Color online) Elliptic flow coefficient for charged particles for different centralities. Stars represent ideal fluid results, reversed triangles, triangles and circles represent the results of vQGP, vHG and vQGP+vHG viscous hydrodynamic calculations respectively. The solid line with squares denotes the results of calculations using  $\eta_{HG}/s = 0.24$ ,  $\eta_{QGP}/s = 0.08$  and the same bulk viscosity as in the scenarios vHG and vQGP+vHG. Data are from the STAR Collab. [64].

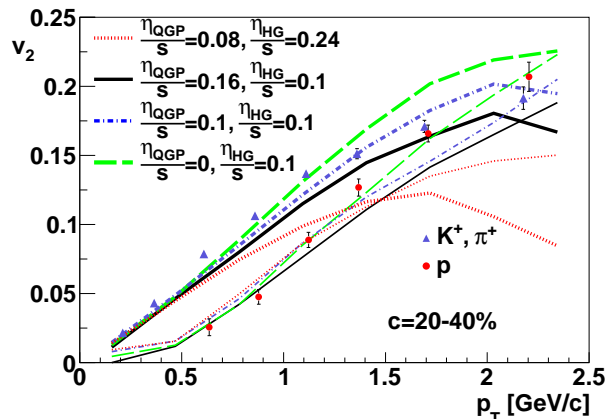


FIG. 10: (Color online) Elliptic flow of mesons (triangles) and protons (circles) as function of transverse momentum [57], compared to model calculations. We present three simulations assuming an increasing shear viscosity to entropy density ratio with decreasing temperature (vHG,  $\eta_{QGP}/s = 0$ ,  $\eta_{HG}/s = 0.1$ , dashed lines), a constant one ( $\eta_{QGP}/s = 0.1$ ,  $\eta_{HG}/s = 0.1$ , dashed-dotted lines) and a decreasing one (vQGP+vHG,  $\eta_{QGP}/s = 0.16$ ,  $\eta_{HG}/s = 0.1$ , solid lines). Also are shown results for a calculation with a minimal QGP viscosity  $\eta_{QGP}/s = 0.08$  and moderately large hadronic viscosity  $\eta_{HG}/s = 0.24$  (dotted lines). Thick and thin lines represent meson and proton elliptic flow respectively.

In Fig. 9 is plotted the average elliptic flow coefficient of charged particles at different centralities. The ideal fluid calculation overpredicts the elliptic flow in peripheral collisions. The discrepancy increases with the impact parameter indicating that corrections to the ideal fluid dynamics should be more important in collisions where the hadronic phase is relatively more important. Comparing the three calculations with viscosities, we find that adding more dissipative mechanism reduces the final elliptic flow. However, the differences between the two scenarios with or without viscosity in the plasma phase are not very big. Most of the effect of the reduction of the azimuthal asymmetry of the flow comes from the hadronic dissipation. One must conclude that the sensitivity of the elliptic flow to the shear viscosity in the early phase is strongly reduced if additional dissipation occurs below  $T_c$ . It must be stressed that the assumed strength of shear viscosity in the hadronic medium is small. We performed also simulations in a scenario with a larger value of the viscosity in the hadron phase  $\eta_{HG}/s = 0.24$ , with  $\eta_{QGP}/s = 0.08$  and a freeze-out temperature of 135MeV. The result is plotted in Fig. 9 (solid line with squares), the elliptic flow of charged particles is below the experimental values, which means that the assumed shear viscosity is too large. This is in line with previous calculations using a constant value of shear viscosity, where the simulations with  $\eta/s = 0.08$  best reproduce the data [67].

In Fig. 10 is presented a direct comparison of the elliptic flow coefficient as function of transverse momentum for different choices of the temperature dependence of the shear viscosity to entropy density ratio. We take three different values of the QGP viscosity  $\eta_{QGP}/s = 0, 0.1$  and  $0.16$  and  $\eta_{HG}/s = 0.1$ . It means that we check three qualitatively different scenarios with  $\eta/s$  increasing, constant or decreasing when the temperature drops below  $T_c$ . The first observation is that the differences between the three calculations are small, moreover increasing  $\eta_{QGP}/s$  always leads to a decrease of the elliptic flow. We find a satisfactory description of the data with a small value of  $\eta_{HG}/s = 0.1$ . For a calculation using a minimal QGP shear viscosity  $\eta_{QGP}/s = 0.08$  and a larger value of  $\eta_{HG} = 0.24$  the calculated final elliptic flow of mesons is significantly below the data. Increasing  $\eta_{QGP}/s$  leads to a decrease of  $v_2$ , also increasing  $\eta_{HG}/s$  from  $0.1$  to  $0.24$  gives a strong reduction of the elliptic flow. Comparing these results to experimental data we obtain the following conclusions: both viscosity effects in the plasma and in the hadronic phase lead to a decrease of  $v_2$ , when choosing a small value of  $\eta_{QGP}/s = 0.08-0.1$  the best results are obtained for a small value of  $\eta_{HG}/s = 0.1$  (and not  $0.24$ ), even if the QGP viscosity is zero the preferred value of the hadronic viscosity is small.

We calculate HBT correlation radii of pions emitted from the fireball in the most central collisions. The two particle correlation function sums all pairs of identical pions with interference effects [69, 70]. For a given total momentum of the pair  $k_{\perp}$  the three-dimensional correla-

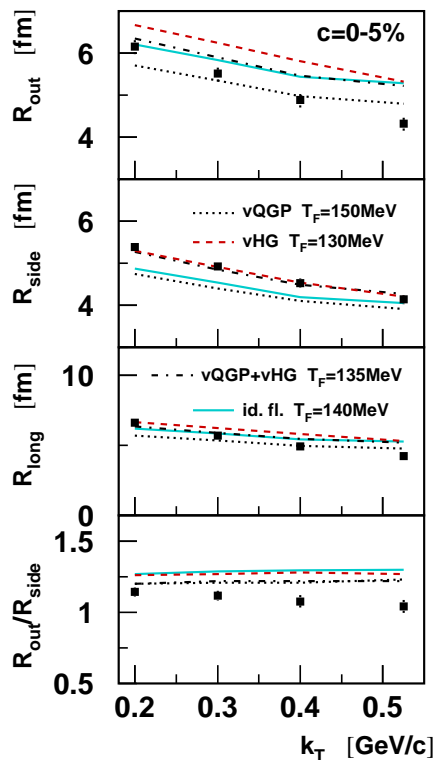


FIG. 11: (Color online) HBT radii for Au-Au collisions at centrality 0 – 5%. Ideal fluid calculation (solid lines), viscous hydrodynamic models vQGP+vHG (dash-dotted lines), vHG (dashed lines), vQGP (dotted lines) and STAR Collab. data [68] (squares) are shown.

tion function in the pion relative momentum is fitted with the Bertsch-Pratt formula [71, 72]. All the scenarios of the hydrodynamic expansion studied lead to HBT radii that are quite close to the data (Fig.11). It is a consequence of the hard equation of state used, with only a minimal softening around  $T_c$  [11]. The scenarios differ by the freeze-out temperatures, a higher freeze-out temperature means a shorter lifetime and hence smaller values of the radii.  $R_{side}$  measuring the geometrical size of the system at freeze-out decreases monotonically with increasing  $T_F$ . The description of the experimentally observed small value of the ratio  $R_{out}/R_{side}$  requires the use of a hard equation of state, early initial time of the expansion, dissipative effects and/or a Gaussian initial profile [11, 73]. Ideal fluid expansion and the expansion with only hadronic dissipation (solid and dashed lines in Fig. 11) give similar results for  $R_{out}/R_{side}$ . The same is true for scenarios with the same viscosity in the early stage but different hadronic dissipation (dotted and dash-dotted lines overlap in the lowest panel in Fig. 11). We can conclude that the ratio  $R_{out}/R_{side}$  is sensitive to the early build up of the transverse flow and is not sensitive to viscosity effects at freeze-out. This is in contrast to the elliptic flow which is sensitive to dissipative effects at all the stages of the expansion. We cannot reproduce exactly the observed HBT radii, this may indicate that

the amount of the early transverse flow in the expansion is too low.

## V. CONCLUSIONS

We present a study of viscosity effects at different stages of the expansion of the fireball created in relativistic heavy ion collisions. We introduce the possibility to have two different shear viscosities in the QGP and hadronic phases of the matter. Assuming zero shear viscosity or  $\eta/s = 0.16$  in the plasma, we test its impact on the final observables. The sensitivity of the final elliptic flow observables to the early viscosity is reduced by the dissipative effects in the hadronic phase. A crucial effect is the introduction of a moderate value of the bulk viscosity in the hadronic medium. Such an assumption is natural in a system with partial equilibration and finite particle masses. The bulk and shear viscosities are treated as free parameters. We use however a relaxation time approximation to relate the values of the shear and bulk viscosities in the hadron gas. A moderate value of the bulk viscosity  $\zeta/s = 0.03-0.04$  corresponds to a relatively small value of the shear viscosity  $\eta/s = 0.1$ . Bulk viscosity in the late stage leads to a shift of the freeze-out temperature to a value allowing for a satisfactory description of the mass ordering of the elliptic flow of identified hadrons without spoiling the agreement in the HBT radii and transverse momentum spectra.

From the simulations using Glauber Model initial densities here presented we can conclude that the shear viscosity in the hadronic phase is in the range  $0.1 < \eta_{HG}/s < 0.24$ . Shear viscosity in the plasma phase leads to a decrease of elliptic flow, but it is the value of  $\eta$  at late stages that is the most important for the suppression of the elliptic flow in all the cases  $\eta_{QGP}/s < \eta_{HG}/s$ ,  $\eta_{QGP}/s = \eta_{HG}/s$ , or  $\eta_{QGP}/s > \eta_{HG}/s$ . Even taking  $\eta_{QGP} = 0$  leads to a preferred value of  $\eta_{HG}/s = 0.1$  that best reproduces the data. Therefore, our results pointing to a small value of the shear viscosity in the hadronic phase, are consistent with previous calculations using the same small value of  $\eta$  in the plasma and in the hadron fluids.

The extracted shear viscosity is significantly below the microscopic estimates of the shear viscosity in the hadronic matter  $\eta_{HG}/s \simeq 1$ . Using  $\eta/s \simeq 1$  in hydrodynamic simulations with the large velocity gradients in heavy-ion collisions is beyond the range of applicability of Israel-Stewart formalism, it would lead to severe numerical instabilities, and is disfavored by elliptic flow data. It is not clear to the author what is the mechanism that prevents the expected large shear viscosity in the hadronic matter to become effective in the viscous hydrodynamic evolution of heavy ion collisions. Before concluding that the hadronic matter is indeed a low viscosity fluid, it should be checked whether the difference between transport model estimates and hydrodynamics is not due to a deficiency of the sudden freeze-out procedure used in the

calculations [74] or to a strong increase of the relaxation time  $\tau_\pi$  below  $T_c$  analogously to what has been discussed for bulk viscosity in Ref. [50].

We find that the elliptic flow coefficient is significantly reduced due to viscosity effects both in the plasma and in the hadronic matter. It means that the extraction of the shear viscosity in QGP is difficult and can be reliably addressed only after precisely constraining the freeze-out conditions. By this we mean determining both the freeze-out temperature and the nonequilibrium effects in the final state. It is interesting to note that the HBT radii have a simple dependence on the choice of the freeze-out. The radii increase for a larger lifetime of the system, caused by a smaller freeze-out temperature. The ratio  $R_{out}/R_{side}$  is almost insensitive to the freeze-out condition, but it depends on the amount of the transverse flow generated in the early phase. One of the mechanism increasing the

early transverse flow is due to the shear viscosity in the plasma phase.

Let us close by repeating the observation that the introduction of bulk viscosity in the hadronic medium changes the freeze-out conditions in the hydrodynamic expansion of the fireball. This allows for a good and simultaneous description of transverse momentum spectra, identified particle elliptic flow and HBT radii.

### Acknowledgments

The author thanks W. Florkowski, U. Heinz, J.-Y. Ollitrault, S. Pratt and D. Teaney for comments and discussion. Supported by Polish Ministry of Science and Higher Education under grant N202 034 32/0918

- 
- [1] I. Arsene et al. (BRAHMS), Nucl. Phys. **A757**, 1 (2005).
  - [2] B. B. Back et al. (PHOBOS), Nucl. Phys. **A757**, 28 (2005).
  - [3] J. Adams et al. (STAR), Nucl. Phys. **A757**, 102 (2005).
  - [4] K. Adcox et al. (PHENIX), Nucl. Phys. **A757**, 184 (2005).
  - [5] D. Teaney, J. Lauret, and E. V. Shuryak, Phys. Rev. Lett. **86**, 4783 (2001).
  - [6] P. F. Kolb and U. W. Heinz, in *Quark Gluon Plasma 3*, edited by R. Hwa and X. N. Wang (World Scientific, Singapore, 2004), nucl-th/0305084.
  - [7] T. Hirano and K. Tsuda, Phys. Rev. **C66**, 054905 (2002).
  - [8] Y. Hama et al., Nucl. Phys. **A774**, 169 (2006).
  - [9] P. Huovinen and P. V. Ruuskanen, Ann. Rev. Nucl. Part. Sci. **56**, 163 (2006).
  - [10] T. Hirano, U. W. Heinz, D. Kharzeev, R. Lacey, and Y. Nara, Phys. Lett. **B636**, 299 (2006).
  - [11] W. Broniowski, M. Chojnacki, W. Florkowski, and A. Kisiel, Phys. Rev. Lett. **101**, 022301 (2008).
  - [12] E. Schnedermann, J. Sollfrank, and U. W. Heinz, Phys. Rev. **C48**, 2462 (1993).
  - [13] P. F. Kolb, J. Sollfrank, and U. W. Heinz, Phys. Rev. **C62**, 054909 (2000).
  - [14] A. Muronga, Phys. Rev. Lett. **88**, 062302 (2002).
  - [15] D. Teaney, Phys. Rev. **C68**, 034913 (2003).
  - [16] R. Baier and P. Romatschke, Eur. Phys. J. **C51**, 677 (2007).
  - [17] P. Romatschke and U. Romatschke, Phys. Rev. Lett. **99**, 172301 (2007).
  - [18] A. K. Chaudhuri, Phys. Rev. **C74**, 044904 (2006).
  - [19] H. Song and U. W. Heinz, Phys. Lett. **B658**, 279 (2008).
  - [20] W. Israel and J. Stewart, Annals Phys. **118**, 341 (1979).
  - [21] P. K. Kovtun, D. T. Son, and A. O. Starinets, Phys. Rev. Lett. **94**, 111601 (2005).
  - [22] L. P. Csernai, J. I. Kapusta, and L. D. McLerran, Phys. Rev. Lett. **97**, 152303 (2006).
  - [23] H. Song and U. W. Heinz, J. Phys. **G36**, 064033 (2009).
  - [24] H. J. Drescher and Y. Nara, Phys. Rev. **C75**, 034905 (2007).
  - [25] P. F. Kolb, U. W. Heinz, P. Huovinen, K. J. Eskola, and K. Tuominen, Nucl. Phys. **A696**, 197 (2001).
  - [26] M. Miller and R. Snellings (2003), nucl-ex/0312008.
  - [27] B. Alver et al. (PHOBOS) (2007), nucl-ex/0701049.
  - [28] P. Bożek, Phys. Rev. **C79**, 054901 (2009).
  - [29] T. Hirano and M. Gyulassy, Nucl. Phys. **A769**, 71 (2006).
  - [30] T. Hirano, Phys. Rev. Lett. **86**, 2754 (2001).
  - [31] T. Hirano, U. W. Heinz, D. Kharzeev, R. Lacey, and Y. Nara, J. Phys. **G34**, S879 (2007).
  - [32] P. Huovinen, Nucl. Phys. **A761**, 296 (2005).
  - [33] S. A. Bass and A. Dumitru, Phys. Rev. **C61**, 064909 (2000).
  - [34] C. Nonaka and S. A. Bass, Phys. Rev. **C75**, 014902 (2007).
  - [35] K. Werner et al., J. Phys. **G36**, 064030 (2009).
  - [36] M. Prakash, M. Prakash, R. Venugopalan, and G. Welke, Phys. Rept. **227**, 321 (1993).
  - [37] N. Demir and S. A. Bass, Phys. Rev. Lett. **102**, 172302 (2009).
  - [38] A. Dobado, F. J. Llanes-Estrada, and J. M. Torres-Rincon, Phys. Rev. **D80**, 114015 (2009).
  - [39] J.-W. Chen and E. Nakano, Phys. Lett. **B647**, 371 (2007).
  - [40] K. Itakura, O. Morimatsu, and H. Otomo, Phys. Rev. **D77**, 014014 (2008).
  - [41] J. Noronha-Hostler, J. Noronha, and C. Greiner, Phys. Rev. Lett. **103**, 172302 (2009).
  - [42] D. Fernández-Fraile and A. Gomez Nicola, Phys. Rev. Lett. **102**, 121601 (2009).
  - [43] M. Chojnacki and W. Florkowski, Acta Phys. Polon. **B38**, 3249 (2007).
  - [44] M. Chojnacki, W. Florkowski, W. Broniowski, and A. Kisiel, Phys. Rev. **C78**, 014905 (2008).
  - [45] A. Hosoya and K. Kajantie, Nucl. Phys. **B250**, 666 (1985).
  - [46] S. Gavin, Nucl. Phys. **A435**, 826 (1985).
  - [47] C. Sasaki and K. Redlich, Phys. Rev. **C79**, 055207 (2009).
  - [48] G. Torrieri et al., Comput. Phys. Commun. **167**, 229 (2005).
  - [49] D. Kharzeev and K. Tuchin, JHEP **09**, 093 (2008).
  - [50] H. Song and U. W. Heinz, Phys. Rev. **C81**, 024905

- (2010).
- [51] G. S. Denicol, T. Kodama, T. Koide, and P. Mota, Phys. Rev. **C80**, 064901 (2009).
- [52] G. Torrieri, B. Tomasik, and I. Mishustin, Phys. Rev. **C77**, 034903 (2008).
- [53] A. Monnai and T. Hirano, Phys. Rev. **C80**, 054906 (2009).
- [54] R. Baier, P. Romatschke, and U. A. Wiedemann, Phys. Rev. **C73**, 064903 (2006).
- [55] K. Dusling, G. Moore, and D. Teaney (2009), arXiv: 0909.0754 [nucl-th].
- [56] S. S. Adler et al. (PHENIX), Phys. Rev. **C69**, 034909 (2004).
- [57] S. S. Adler et al. (PHENIX), Phys. Rev. Lett. **91**, 182301 (2003).
- [58] J. Cleymans, B. Kampfer, M. Kaneta, S. Wheaton, and N. Xu, Phys. Rev. **C71**, 054901 (2005).
- [59] P. Bozek, Acta Phys. Polon. **B36**, 3071 (2005).
- [60] F. Becattini and J. Manninen, Phys. Lett. **B673**, 19 (2009).
- [61] P. Braun-Munzinger, D. Magestro, K. Redlich, and J. Stachel, Phys. Lett. **B518**, 41 (2001).
- [62] W. Florkowski, W. Broniowski, and M. Michalec, Acta Phys. Polon. **B33**, 761 (2002).
- [63] J. Adams et al. (STAR), Phys. Rev. Lett. **95**, 122301 (2005).
- [64] J. Adams et al. (STAR), Phys. Rev. **C72**, 014904 (2005).
- [65] T. Hirano, U. W. Heinz, D. Kharzeev, R. Lacey, and Y. Nara, Phys. Rev. **C77**, 044909 (2008).
- [66] A. K. Chaudhuri (2009), arXiv: 0909.0376 [nucl-th].
- [67] M. Luzum and P. Romatschke, Phys. Rev. **C78**, 034915 (2008).
- [68] J. Adams et al. (STAR), Phys. Rev. **C71**, 044906 (2005).
- [69] A. Kisiel, W. Florkowski, W. Broniowski, and J. Pluta, Phys. Rev. **C73**, 064902 (2006).
- [70] A. Kisiel, Braz. J. Phys. **37**, 917 (2007).
- [71] S. Pratt, Phys. Rev. **D33**, 72 (1986).
- [72] G. F. Bertsch, Nucl. Phys. **A498**, 173c (1989).
- [73] S. Pratt, Phys. Rev. Lett. **102**, 232301 (2009).
- [74] P. Huovinen and D. Molnar, Phys. Rev. **C79**, 014906 (2009).